Exceptional points in the scattering continuum

J. Okołowicz[1] and M. Płoszajczak[2]

[1]*Institute of Nuclear Physics, Polish Academy of Sciences, Radzikowskiego 152, PL-31342 Kraków, Poland*

[2]*Grand Accélérateur National d'Ions Lourds (GANIL), CEA/DSM-CNRS/IN2P3, BP 5027, F-14076 Caen Cedex 05, France*

(Received 9 June 2009; revised manuscript received 31 July 2009; published 30 September 2009)

The manifestation of exceptional points in the scattering continuum of an atomic nucleus is studied using the real-energy continuum shell model. It is shown that low-energy exceptional points appear for realistic values of coupling to the continuum and, hence, could be accessible experimentally. Experimental signatures are proposed which include the jump by 2π of the elastic scattering phase shift and a salient energy dependence of cross sections in the vicinity of the exceptional point.

DOI: 10.1103/PhysRevC.80.034619 PACS number(s): 25.70.Ef, 03.65.Vf, 21.60.Cs, 25.40.Cm

I. INTRODUCTION

The structure of loosely bound and unbound nuclei is strongly impacted by many-body correlations and nonperturbative coupling to the external environment of scattering states and decay channels [1,2]. This is particularly important in exotic nuclei where new phenomena, at the borderline of nuclear structure and nuclear reactions, are expected. Some of them, such as the halos [3], the segregation of time scales in the context of non-Hermitian Hamiltonians [4], the alignment of near-threshold states with decay channels [5], and the resonance crossings [6,7], appear in various *open* mesoscopic systems. Their universality is the consequence of the non-Hermitian nature of an eigenvalue problem in open quantum systems.

Resonances are commonly found in quantum systems independently of their interactions, building blocks, and energy scales involved. Much interest is concentrated on resonance degeneracies, the so-called exceptional points (EPs) [6]. Their connection to avoided crossings and spectral properties of Hermitian systems [8,9] as well as the associated geometric phases have been discussed in simple models in considerable detail [10]. The interesting question is their manifestation in nuclear scattering experiments. Here, a much studied case was the 2^+ doublet in ^{8}Be [11–15]. Based on this example, von Brentano [16] discussed the width attraction for mixed resonances, and Hernandéz and Mondragón [17] showed that the true crossing of resonances can be obtained by the variation of two parameters in the Jordan block of rank two. In this latter analysis, it was shown that the resonating part of the scattering matrix (S matrix) for one open channel and two internal states is compatible with the two-level formula of the R-matrix theory used in the experimental analysis of excitation functions of elastic scattering ^{4}He(α,α_0)^{4}He [15] and, hence, the 2^+ doublet in ^{8}Be may actually be close to the true resonance degeneracy.

Properties of the atomic nucleus around the continuum threshold change rapidly with the nucleon number, the excitation energy, and the coupling to the environment of scattering states. A consistent description of the interplay between scattering and resonant states requires an open system formulation of the nuclear shell model (see [1,2,18] for recent reviews). The real-energy continuum shell model [19–21] provides a suitable unified framework with the help of an effective non-Hermitian Hamiltonian. In this work, for the first time we focus on a realistic model of an unbound atomic nucleus to see whether one or more EPs can appear in the low energy continuum for sensible parameters of the open quantum system Hamiltonian. In particular, we discuss possible experimental signatures of the EPs and show the evolution of these signatures in the vicinity of the EP. Finally, on the example of spectroscopic factors we demonstrate the entanglement of resonance wave functions close to the EP.

II. FORMULATION OF THE CONTINUUM SHELL MODEL

Let us briefly review the shell model embedded in the continuum (SMEC) [21], which is a recent realization of the real-energy continuum shell model. The total function space of an A-particle system consists of the set of square-integrable functions $\mathcal{Q} \equiv \{\psi_i^A\}$, used in the standard nuclear shell model (SM), and the set of embedding scattering states $\mathcal{P} \equiv \{\zeta_E^c\}$. These two sets are obtained by solving the Schrödinger equation separately for discrete (SM) states (the closed quantum system) and for scattering states (the environment). Decay channels 'c' are determined by the motion of an unbound particle in a state l_j relative to the $A-1$ nucleus with all nucleons on bounded single-particle (s.p.) orbits in the SM eigenstate ψ_j^{A-1}. Using these function sets, one defines projection operators:

$$\hat{Q} = \sum_{i=1}^{N} |\psi_i^A\rangle\langle\psi_i^A|; \quad \hat{P} = \int_0^\infty dE |\zeta_E\rangle\langle\zeta_E|$$

and projected Hamiltonians: $\hat{Q}H\hat{Q} \equiv H_{QQ}$, $\hat{P}H\hat{P} \equiv H_{PP}$, $\hat{Q}H\hat{P} \equiv H_{QP}$, $\hat{P}H\hat{Q} \equiv H_{PQ}$. Assuming $\mathcal{Q}+\mathcal{P} = \mathcal{I}$, one can determine the third set of functions $\{\omega_i^{(+)}\}$ which contains the continuation of any SM eigenfunction ψ_i^A in $\mathcal{P}$, and then construct the complete solution in $\mathcal{Q}+\mathcal{P}$ [1]. Recently, this approach has been extended to describe the two-proton radioactivity with the two-particle continuum [22].

Open quantum system solutions in $\mathcal{Q}$, which include couplings to the environment of scattering states and decay channels, are obtained by solving the eigenvalue problem for

the energy-dependent effective Hamiltonian:

$$\mathcal{H}_{QQ}(E) = H_{QQ} + H_{QP}G_P^{(+)}(E)H_{PQ},$$

where H_{QQ} is the closed system Hamiltonian, $G_P^{(+)}(E)$ is the Green function for the motion of a single nucleon in $\mathcal{P}$ subspace and E is the energy of this nucleon (the scattering energy). Index '+' in $G_P^{(+)}$ stands for the outgoing boundary in the scattering problem. $\mathcal{H}_{QQ}$ is non-Hermitian for unbound states and its eigenstates $|\Phi_\alpha\rangle$ are linear combinations of SM eigenstates $|\psi_i\rangle$. The eigenstates of $\mathcal{H}_{QQ}$ are biorthogonal; the left $|\Phi_\alpha\rangle$ and right $|\Phi_{\bar{\alpha}}\rangle$ eigenstates have the wave functions related by the complex conjugation. The orthonormality condition in the biorthogonal basis reads $\langle\Phi_{\bar{\alpha}}|\Phi_\beta\rangle = \delta_{\alpha,\beta}$. Similarly, the matrix element of an operator $\hat{O}$ is $O_{\alpha\beta} = \langle\Phi_{\bar{\alpha}}|\hat{O}|\Phi_\alpha\rangle$.

The scattering function Ψ_E^c is a solution of a Schrödinger equation in the total function space:

$$\Psi_E^c = \zeta_E^c + \sum_\alpha a_\alpha \tilde{\Phi}_\alpha,$$

where

$$a_\alpha \equiv \langle\Phi_\alpha|H_{QP}|\zeta_E^c\rangle/(E - \mathcal{E}_\alpha)$$

and

$$\tilde{\Phi}_\alpha \equiv (1 + G_P^{(+)}H_{PQ})\Phi_\alpha.$$

Inside of an interaction region, the dominant contributions to Ψ_E^c are given by eigenfunctions Φ_α of the effective non-Hermitian Hamiltonian [1]:

$$\Psi_E^c \sim \sum_\alpha a_\alpha \Phi_\alpha.$$

For bounds states, eigenvalues $\mathcal{E}_\alpha(E)$ of $\mathcal{H}_{QQ}(E)$ are real and $\mathcal{E}_\alpha(E) = E$. For unbound states, physical resonances can be identified with the narrow poles of the S matrix [2,23], or using the Breit-Wigner approach which leads to a fixed-point condition [1,18,24]:

$$E_\alpha = \mathrm{Re}\left(\mathcal{E}_\alpha(E)\right)|_{E=E_\alpha}; \quad \Gamma_\alpha = -2\,\mathrm{Im}\left(\mathcal{E}_\alpha(E)\right)|_{E=E_\alpha}. \quad (1)$$

Here it is assumed that the origin of $\mathrm{Re}(\mathcal{E})$ is fixed at the lowest particle emission threshold.

An EP is a generic phenomenon in Hamiltonian systems. In our case, the EP can appear as a result of the continuum-coupling term $H_{QP}G_P^{(+)}(E)H_{PQ}$ for energies above the first particle emission threshold ($E > 0$). The eigenvalue degeneracies are indicated by common roots of two equations [6]:

$$\frac{\partial^{(\nu)}}{\partial\mathcal{E}}\det[\mathcal{H}_{QQ}(E;V_0) - \mathcal{E}I] = 0, \quad \nu = 0, 1. \quad (2)$$

Single-root solutions of Eq. (2) correspond to EPs associated with decaying states. The maximal number of those roots is $M_{\max} = n(n-1)$, where n is the number of states of given angular momentum J and parity π. In quantum integrable models with at least two parameter-dependent integrals of motion one finds also double-root solutions which correspond to a nonsingular crossing of two levels with two different wave functions. Hence, the actual number of EPs in these systems is always smaller than $M_{\max}$ [9].

The position of EPs in the spectrum of eigenvalues of $\mathcal{H}_{QQ}$ depends both on the chosen interaction and the energy E of the system. In general, eigenvalues of the energy-dependent effective Hamiltonian $\mathcal{H}_{QQ}(E)$ need not satisfy the fixed-point condition (1) and hence need not correspond to poles of the S matrix (resonances). In the following, we shall consider uniquely the case where EPs are *identical* with double poles of the S matrix.

III. EXCEPTIONAL POINTS IN THE SCATTERING CONTINUUM OF ^{16}Ne

Let us investigate properties of EPs on the example of ^{16}Ne. SM eigenstates in this nucleus correspond to a complicated mixture of configurations associated with the dynamics of the ^{16}O core. Our goal is to see if EPs can be possibly found in the scattering continuum of atomic nucleus at low excitation energies and for physical strength of the continuum coupling. SMEC calculations are performed in $p_{1/2}, d_{5/2}, s_{1/2}$ model space. For H_{QQ} we take the ZBM Hamiltonian [25] which correctly describes the configuration mixing around the $N = Z = 8$ shell closure. The residual coupling H_{QP} between $\mathcal{Q}$ and the embedding continuum $\mathcal{P}$ is generated by the contact force: $H_{QP} = H_{PQ} = V_0\delta(r_1 - r_2)$. For each J^π, the SM states $|\psi_i(J^\pi)\rangle$ of the closed quantum system are interconnected via the coupling to common decay channels $[^{15}\mathrm{F}(K^\pi) \otimes \mathrm{p}_{l_j}]^{J^\pi}_{E'}$ with $K^\pi = 1/2^+, 5/2^+$, and $1/2^-$ which have the thresholds at $E = 0$ (the elastic channel), 0.67 MeV, and 2.26 MeV, respectively. In the ZBM model space, these are all possible one-proton ($1p$) decay channels in ^{16}Ne.

The size of a non-Hermitian correction to H_{QQ} depends on two real parameters: the strength V_0 of the continuum coupling in H_{QP} (H_{PQ}) and the system energy E. The range of relevant V_0 values can be determined, for example, by fitting decay widths of the lowest states in ^{15}F. For the present Hamiltonian, experimental decay widths of the ground state $1/2^+_1$ and the first excited state $5/2^+_1$ in ^{15}F are reproduced using $V_0 = -3500 \pm 450$ MeV fm^3 and $V_0 = -1100 \pm 50$ MeV fm^3, respectively. The error bars in V_0 reflect experimental uncertainties of those widths. The weak dependence of $1p$ decay widths on the sign of V_0 is generated by the channel-channel coupling and disappears in a single-channel case.

Figure 1 shows energies E and strengths V_0 which correspond to $J^\pi = 1^-$ EPs in the scattering continuum of ^{16}Ne. Decay channels $[^{15}\mathrm{F}(K^\pi) \otimes \mathrm{p}_{l_j}]^{1^-}_{E'}$ with $K^\pi = 1/2^+, 5/2^+$, and $1/2^-$ have been included with proton partial waves: $p_{1/2}$, $p_{3/2}$ for $K^\pi = 1/2^+$, $p_{3/2}$, $f_{5/2}$, $f_{7/2}$ for $K^\pi = 5/2^+$, and $s_{1/2}$, $d_{3/2}$ for $K^\pi = 1/2^-$. The number of 1^- SM states is 3 and, hence, the maximal number of 1^- EPs in SMEC could be 6. Indeed, all of them exist at $E < 20$ MeV in a physical range of V_0 values (1100 MeV fm^3 $< |V_0| <$ 3500 MeV fm^3). They have been found by scanning the energy dependence of all eigenvalues over a certain range of V_0, searching for all real-energy crossings or width crossings (avoided crossings). Once found, we have tuned V_0 to find out whether these crossings evolve into EPs at some combination of V_0 and E. One should stress that the passage through EP always occurs

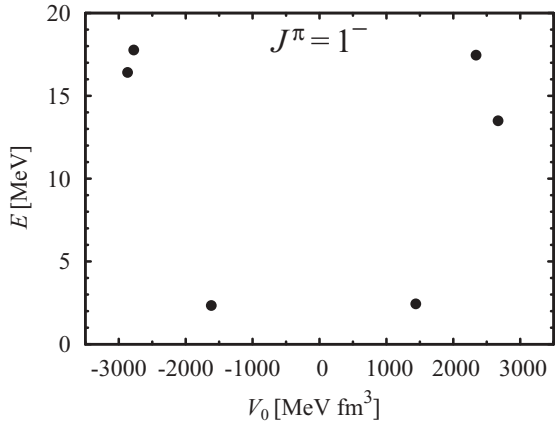

FIG. 1. The map of $J^\pi = 1^-$ exceptional points in the continuum of ^{16}Ne as found in SMEC. For more details, see the description in the text.

if, e.g., the real-energy crossing moves toward $E = 0$. Since such a crossing cannot move into the region $E < 0$, therefore it converts into an avoided crossing via the formation of an EP.

The lowest EP in Fig. 1 is seen at $V_0^{(\mathrm{cr})} = -1617.4$ MeV fm^3 and $E = 2.33$ MeV. This EP corresponds to a degeneracy of the first two 1^- eigenvalues of $\mathcal{H}_{QQ}$ for $V_0 < 0$.

Energy E_i and width Γ_i of 1^-_1 and 1^-_2 eigenvalues are shown in Fig. 2 as a function of the scattering energy. For $E > 2.33$ MeV, the widths of these two eigenvalues grow apart very fast. $E_1(E)$ (solid line) and $E_2(E)$ (dotted line) cross again for $E \simeq 3.2$ MeV. At this energy, Γ_1 and Γ_2 are different and, hence, the corresponding eigenfunctions are different as well.

The upper part of Fig. 2 shows the phase shifts δ_{l_j} for $p + {}^{15}$F elastic scattering as a function of the proton energy for $p_{1/2}$ (dashed-dotted line) and $p_{3/2}$ (dashed line) partial waves. In the partial wave $p_{1/2}$, the elastic scattering phase shift exhibits a jump by 2π at the EP with $J^\pi = 1^-$. This unusual jump in the elastic scattering phase shift is an unmistakable and robust signal of a double-pole of the S matrix (EP) which persists also in its neighborhood, as shall be discussed below.

Figure 3 shows the elastic and inelastic cross sections for $^{15}\mathrm{F}(p, p')$ in the vicinity of an EP. The solid line represents a sum of different partial contributions of both parities with $J \leqslant 5$ whereas the dashed line shows the resonance part of the 1^- contribution in these cross sections. The cross sections are plotted as a function of the center-of-mass scattering energy for $V_0^{(\mathrm{cr})} = -1617.4$ MeV fm^3. The elastic cross section at the EP shows a characteristic double-hump shape [26] with asymmetric tails in energy. The inelastic cross section in this case exhibits a single peak. Both inelastic channels $[{}^{15}\mathrm{F}(5/2^+) \otimes p_{l_j}]^{1^-}_{E'}$ and $[{}^{15}\mathrm{F}(1/2^-) \otimes p_{l_j}]^{1^-}_{E'}$ are opened at the EP. A substantial background contribution to both cross sections comes from broad resonances, mainly 0^+ and 2^+. A sharp peak at $E \simeq 1.65$ MeV corresponds to an ordinary resonance 2^-.

The above discussion of the double poles of the S matrix (EPs) and their manifestation in the many-body scattering continuum concerns 1^- states. The same analysis for $J^\pi =$

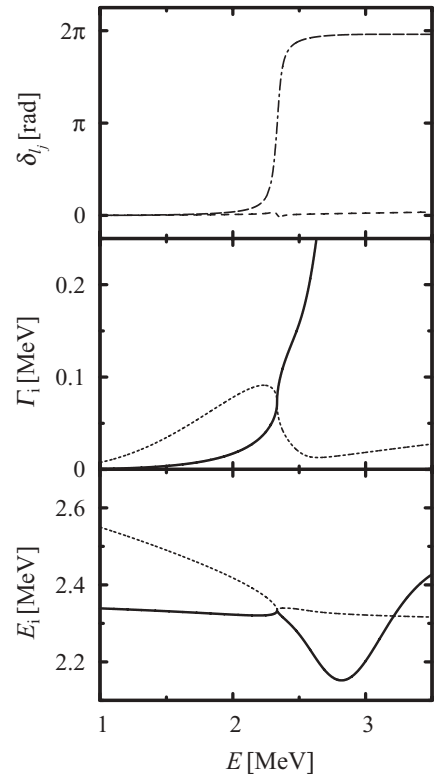

FIG. 2. The upper plot exhibits the elastic scattering phase shifts $\delta_{p_{1/2}}$ (dashed-dotted line) and $\delta_{p_{3/2}}$ (dashed line) for $p + {}^{15}$F reaction in 1^- partial waves at around the EP (the double-pole of the S matrix) with $J^\pi = 1^-$. Lower plots show real and imaginary parts of 1^-_1 (solid line) and 1^-_2 (dotted line) eigenvalues of the effective Hamiltonian $\mathcal{H}_{QQ}(E)$ as a function of the scattering energy E. For other details, see the description in the text.

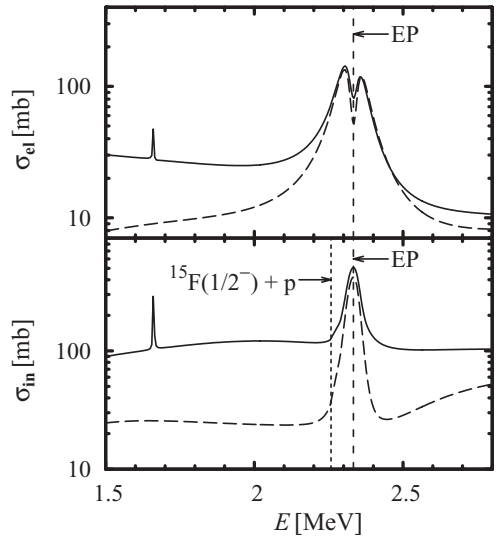

FIG. 3. Elastic and inelastic cross sections in the reaction $^{15}\mathrm{F}(p, p')$ as a function of the proton energy E at around the EP (the double-pole of the S matrix) with $J^\pi = 1^-$ for 1^- resonances only (dashed line) and for all resonances with $J \leqslant 5$ (solid line). For more details, see the description in the text.

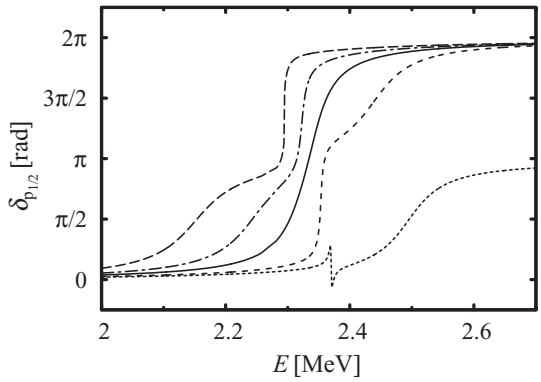

FIG. 4. The elastic scattering phase shifts $\delta_{p_{1/2}}$ for the $p + {}^{15}\mathrm{F}$ reaction in 1^- partial waves at around the EP (the double pole of the S matrix) with $J^\pi = 1^-$ at $V_0^{(\mathrm{cr})} = -1617.4$ MeV fm^3 (solid line). Different curves correspond to different strength V_0 of the continuum coupling: $V_0 = -1800$ MeV fm^3 (long-dashed line), -1700 MeV fm^3 (dashed-dotted line), -1500 MeV fm^3 (short-dashed line), and -1430 MeV fm^3 (dotted line).

0^+, 2^+ states of ^{16}Ne gives qualitatively similar results. Also in these two cases, the number of EPs is maximal but only a fraction of them appears in the relevant range of E and V_0 values.

A. Behavior of scattering wave functions in the vicinity of the exceptional point

A true crossing of two resonant states is accidental and, hence, improbable in nuclear scattering experimentation. In this section, we will investigate the behavior of scattering states in the vicinity of an EP (the double pole of the S matrix) as the observation of such a situation is more plausible.

Figure 4 exhibits the phase shifts δ_{l_j} for $p + {}^{15}\mathrm{F}$ elastic scattering as a function of the proton energy for various values of the strength $V_0 (V_0 = -1800$ MeV fm^3 (long-dashed line), -1700 MeV fm^3 (dashed-dotted line), -1617.4 MeV fm^3 (solid line), -1500 MeV fm^3 (short-dashed line), and -1430 MeV fm^3 (dotted line) of the residual coupling $H_{QP} = H_{PQ} = V_0 \delta(r_1 - r_2)$ between $\mathcal{Q}$ and $\mathcal{P}$ subspaces. The characteristic change by a 2π of the elastic phase shift is seen in a broad interval -1800 MeV fm$^3 \leqslant V_0 \leqslant -1500$ MeV fm^3 of the continuum coupling strength.

Figures 5 and 6 show energies E_i and widths Γ_i of 1_1^- and 1_2^- eigenvalues as a function of the scattering energy for two values of V_0 : -1700 MeV fm^3 (Fig. 5) and -1700 MeV fm^3 (Fig. 6).

The case shown in Fig. 5 corresponds to a subcritical coupling where two resonances cross freely in energy and repel in width [27]. In this regime, the scattering energy E corresponding to the closest approach of 1^- eigenvalues in the complex plane ($E \simeq 2.47$ MeV) is higher than the scattering energy corresponding to the EP at a critical coupling $V_0^{(\mathrm{cr})} = -1617.4$ MeV fm^3. Nevertheless, the elastic scattering phase shift shows the jump by 2π at the position of the EP and not at the point of the closest approach of eigenvalues.

Figure 6 shows the situation corresponding to an overcritical coupling where two resonances exhibit level repulsion in

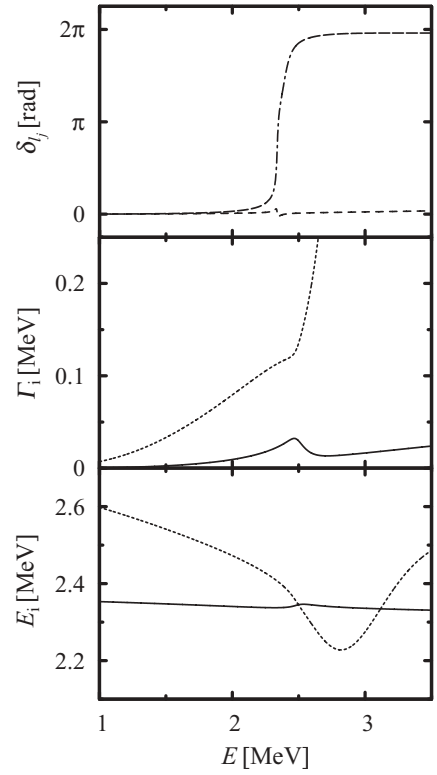

FIG. 5. The same as in Fig. 2 but in the subcritical regime of coupling ($V_0 = -1560$ MeV fm^3). For more details, see the caption of Fig. 2 and the description in the text.

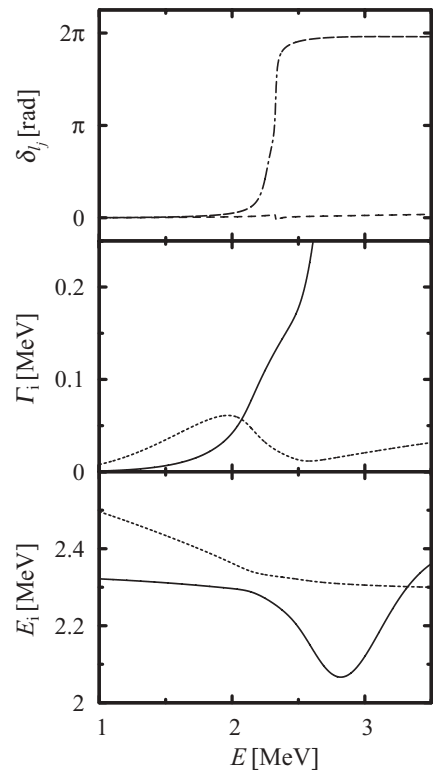

FIG. 6. The same as in Fig. 2 but in the overcritical regime of coupling ($V_0 = -1680$ MeV fm^3). For more details, see the caption of Fig. 2 and the description in the text.

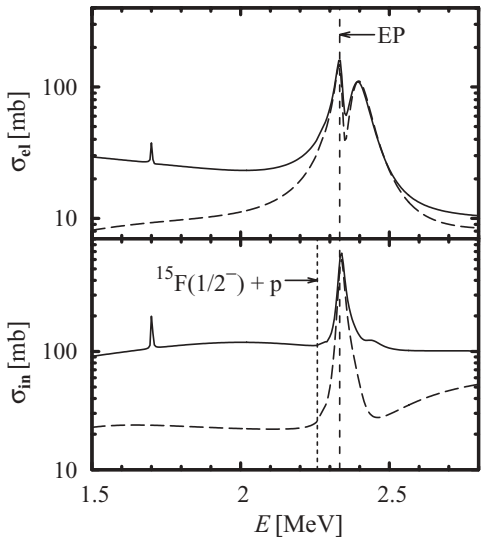

FIG. 7. The same as in Fig. 3 but in the subcritical regime of coupling ($V_0 = -1560$ MeV fm^3). For more details, see the caption of Fig. 2 and the description in the text.

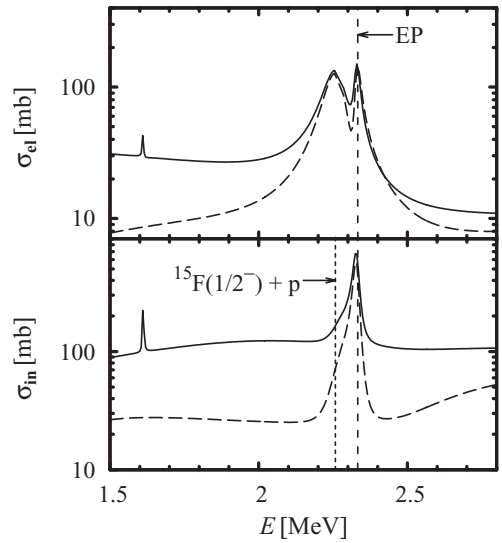

FIG. 8. The same as in Fig. 3 but in the overcritical regime of coupling ($V_0 = -1680$ MeV fm^3). For more details, see the caption of Fig. 2 and the description in the text.

energy and a free crossing of their widths [27]. In this case, the point of the closest approach of 1^- eigenvalues in the complex plane is found at the scattering energy ($E = 2.13$ MeV) which is lower than the corresponding energy for the EP. Again, the elastic scattering phase shift shows the jump by 2π at the position of the double pole.

From these two examples, one can see that the characteristic jump by 2π of the elastic scattering phase shift remains a robust signature of the EP in all close-to-critical regimes of the coupling to the continuum: the subcritical coupling ($|V_0| < |V_0^{(\mathrm{cr})}|$), the critical coupling ($|V_0| = |V_0^{(\mathrm{cr})}|$), and the overcritical coupling ($|V_0| > |V_0^{(\mathrm{cr})}|$), where real and/or imaginary parts of two eigenvalues coincide.

The next two figures show the elastic and inelastic cross sections for $^{15}\mathrm{F}(p,p')$ in the vicinity of the EP with $J^\pi = 1^-$ in the subcritical (Fig. 7) and overcritical (Fig. 8) regimes of the continuum coupling. The curves shown by solid lines in Figs. 7 and 8 represent a sum of different partial contributions of both parities with $J \leqslant 5$. The curves shown by dashed lines exhibit the resonance part of 1^- contribution in these cross sections. The qualitative features of the cross sections for the subcritical ($V_0 = -1560$ MeV fm^3) and overcritical ($V_0 = -1680$ MeV fm^3) couplings remain the same as for the critical coupling (see Fig. 3). In both cases, one sees a double-hump shape in the elastic cross sections and a single-hump shape in the inelastic cross section. One observes also a strong asymmetry in the widths and heights of two peaks and a small shift of the position of the interference minimum in between the two peaks with respect to the energy which the EP is found for a critical coupling.

B. Entangled eigenstates of the effective Hamiltonian

Complex and biorthogonal eigenstates of the effective non-Hermitian Hamiltonian provide a convenient basis in which the resonant part of the scattering function can be expressed. These eigenstates are obtained by an orthogonal and, in general, nonunitary transformation of SM eigenstates [1] which is a consequence of their mixing via coupling to common decay channels. The same coupling is responsible for the entanglement of two eigenstates involved in building of an EP, as illustrated in Fig. 9 on the example of spectroscopic factors.

Figure 9 exhibits the real part of the spectroscopic factor $\mathrm{Re}(S^2) = \mathrm{Re}(\langle ^{16}\mathrm{Ne}(1_n^-)|[^{15}\mathrm{F}(1/2_1^+) \otimes p(0p_{1/2})]^{1^-}\rangle^2)$ in ^{16}Ne in three regimes of the continuum coupling: (a) the subcritical regime ($V_0 = -1560$ MeV fm^3), (b) the critical regime ($V_0^{(\mathrm{cr})} = -1617.4$ MeV fm^3), and (c) the overcritical regime ($V_0 = -1680$ MeV fm^3). The solid (short-dashed) lines show the spectroscopic factors for $\Phi(1_1^-)(E)$ ($\Phi(1_2^-)(E)$) eigenvalues of the effective Hamiltonian $\mathcal{H}_{QQ}(E)$ as a function of the scattering energy E. For a critical coupling [plot (b)], the spectroscopic factors for $\Phi(1_1^-)$ and $\Phi(1_2^-)$ wave functions diverge at the EP (the double pole of the S matrix) but their sum (long-dashed line in Fig. 9) remains finite and constant over a whole region of scattering energies surrounding the EP. In that sense, $\Phi(1_1^-)$ and $\Phi(1_2^-)$ resonance wave functions form an inseparable doublet of eigenfunctions with entangled spectroscopic factors. This entanglement is a direct consequence of the energy dependence of coefficients $b_{\alpha i}$:

$$|\Phi_\alpha\rangle = \sum_i b_{\alpha i}(E)|\psi_i\rangle,$$

in a decomposition of $\mathcal{H}_{QQ}(E)$ eigenstates in the basis of SM eigenstates.

One may notice that the energy dependence of $\mathrm{Re}(S^2)$ in the vicinity of the double pole for 1_1^- and 1_2^- eigenstates is quite different in all three regimes of the continuum coupling. In particular, in the overcritical regime of coupling, an EP yields entangled states in a broad range of scattering energies. The

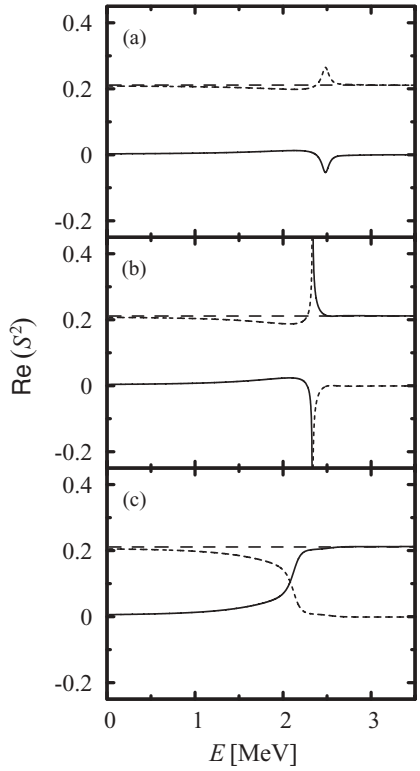

FIG. 9. $p_{1/2}$-spectroscopic factor $\langle^{16}\mathrm{Ne}(1_n^-)|[^{15}\mathrm{F}(1/2_1^+)\otimes p(0p_{1/2})]^{1^-}\rangle$ for 1_1^- and 1_2^- eigenvalues of the effective Hamiltonian at around the double pole of the S matrix. For more details, see the discussion in the text.

strongest entanglement is found at the scattering energy which corresponds to the point of the closest approach of eigenvalues in the complex plane for all regimes of coupling. Obviously, the entanglement of resonance eigenfunctions in the vicinity of an EP is a generic phenomenon in open quantum systems which is manifested in matrix elements and expectation values for any operator which does not commute with the Hamiltonian.

IV. CONCLUSIONS

In conclusion, we have shown in SMEC studies of the one-nucleon continuum that EPs exist for realistic values of the continuum coupling strength. In the studied case of ^{16}Ne, few of those EPs appear at sufficiently low excitation energies to be seen in the excitation function as individual peaks associated with a jump by 2π of the elastic scattering phase shift. The occurrence of an EP leaves also characteristic imprints in its neighborhood, i.e., for avoided crossing of resonances. In all close-to-critical regimes of the continuum coupling where real and/or imaginary parts of the two eigenvalues coincide, one finds qualitatively similar features of the elastic scattering phase shift and the elastic cross section as found for the critical coupling at around the EP (the double pole of the S matrix). This gives a real chance that EPs or their traces may actually be searched for experimentally in the atomic nucleus. The well-known case of 2^+ doublet in ^{8}Be, where resonance energies and widths are 16623 ± 3 keV, 107 ± 0.5 keV, and 16925 ± 3 keV, 74.4 ± 0.4 keV, respectively [15], nearly satisfies the resonance conditions in the close-to-critical regime of couplings. Various situations in this regime have been studied experimentally in the microwave cavity [27].

Avoided crossing of two resonances with the same quantum numbers provide the valuable information about the configuration mixing in open quantum systems. As the formation of any EP in the scattering continuum depends on a subtle interplay between the internal Hamiltonian (H_{QQ}) and the coupling to the external environment of decay channels, its finding provides a stringent test of an effective nucleon-nucleon interaction and the configuration mixing in the open quantum system regime. Such tests are crucial for a quantitative description of atomic nuclei in the vicinity of drip lines.

ACKNOWLEDGMENT

We wish to thank J. Dukelsky and W. Nazarewicz for stimulating discussions and suggestions.

[1] J. Okołowicz, M. Płoszajczak, and I. Rotter, Phys. Rep. **374**, 271 (2003).
[2] N. Michel, W. Nazarewicz, M. Płoszajczak, and T. Vertse, J. Phys. G: Nucl. Part. Phys. **36**, 013101 (2009).
[3] K. Riisager, D. V. Fedorov, and A. S. Jensen, Europhys. Lett. **49**, 547 (2000).
[4] P. Kleinwächter and I. Rotter, Phys. Rev. C **32**, 1742 (1985); E. Persson, I. Rotter, H.-J. Stöckmann, and M. Barth, Phys. Rev. Lett. **85**, 2478 (2000).
[5] K. Ikeda, N. Takigawa, and H. Horiuchi, Prog. Theor. Phys. Suppl. Extra Number, 464 (1968); A. I. Baz'*et al.*, *Scattering, Reactions and Decay in Nonrelativistic Quantum Mechanics* (IPST, 1969); R. Chatterjee, J. Okołowicz, and M. Płoszajczak, Nucl. Phys. **A764**, 528 (2006).
[6] M. R. Zirnbauer, J. J. M. Verbaarschot, and H. A. Weidenmüller, Nucl. Phys. **A411**, 161 (1983).
[7] W. D. Heiss and W.-H. Steeb, J. Math. Phys. **32**, 3003 (1991).
[8] W. D. Heiss and A. L. Sannino, Phys. Rev. A **43**, 4159 (1991).
[9] J. Dukelsky, J. Okołowicz, and M. Płoszajczak, J. Stat. Mech. (2009) L07001.
[10] W. D. Heiss, M. Müller, and I. Rotter, Phys. Rev. E **58**, 2894 (1998); W. D. Heiss, *ibid.* **61**, 929 (2000); C. Dembowski, H. D. Graf, H. L. Harney, A. Heine, W. D. Heiss, H. Rehfeld, and A. Richter, Phys. Rev. Lett. **86**, 787 (2001); C. Dembowski, B. Dietz, H. D. Graf, H. L. Harney, A. Heine, W. D. Heiss, and A. Richter, *ibid.* **90**, 034101 (2003); F. Keck, H. J. Korsch, and S. Mossmann, J. Phys. A **36**, 2125 (2003).
[11] J. B. Marion, Phys. Lett. **14**, 315 (1965).
[12] P. Paul, Z. Naturforsch. **21a**, 914 (1966).
[13] F. C. Barker, Nucl. Phys. **83**, 418 (1966).
[14] C. P. Browne, W. D. Callender, and J. Erskine, Phys. Lett. **23**, 371 (1966).
[15] F. Hinterberger, P. D. Eversheim, P. von Rossen, B. Schűller, R. Schőnhagen, M. Thenée, R. Gőrgen, T. Braml, and H. J. Hartmann, Nucl. Phys. **A299**, 397 (1978).

[16] P. von Brentano, Phys. Lett. **B246**, 320 (1990); P. von Brentano and R.-D. Herzberg, *ibid.* **B265**, 14 (1991).
[17] E. Hernández and A. Mondragón, Phys. Lett. **B326**, 1 (1994).
[18] A. Volya and V. Zelevinsky, Phys. Rev. C **74**, 064314 (2006).
[19] H. Feshbach, Ann. Phys. (NY) **5**, 357 (1958); **19**, 287 (1962).
[20] U. Fano, Phys. Rev. **124**, 1866 (1961); C. Mahaux and H. A. Weidenműller, *Shell Model Approach to Nuclear Reactions* (North Holland, Amsterdam, 1969); H. W. Barz, I. Rotter, and J. Höhn, Nucl. Phys. **A275**, 111 (1977).
[21] K. Bennaceur, F. Nowacki, J. Okołowicz, and M. Płoszajczak, Nucl. Phys. **A651**, 289 (1999).
[22] J. Rotureau, J. Okołowicz, and M. Płoszajczak, Nucl. Phys. **A767**, 13 (2006).
[23] A. F. J. Siegert, Phys. Rev. **56**, 750 (1939); T. Berggren, Nucl. Phys. **A109**, 265 (1968).
[24] R. de la Madrid, Eur. J. Phys. **26**, 287 (2005).
[25] A. P. Zuker, B. Buck, and J. B. McGrory, Phys. Rev. Lett. **21**, 39 (1968).
[26] M. Müller, F. M. Dittes, W. Iskra, and I. Rotter, Phys. Rev. E **52**, 5961 (1995); I. Rotter, *ibid.* **68**, 016211 (2003).
[27] M. Philipp, P. von Brentano, G. Pascovici, and A. Richter, Phys. Rev. E **62**, 1922 (2000).